The Journal of Neuroscience, December 1987, 7(12): 4044–4053

Rapid Axonal Transport in Focally Demyelinated Sciatic Nerve

Regina Armstrong,[1,2] Arrel D. Toews,[1,3] and Pierre Morell[1–3]

[1]Biological Sciences Research Center, [2]Curriculum in Neurobiology, and [3]Department of Biochemistry and Nutrition, University of North Carolina, Chapel Hill, North Carolina 27514

Focal demyelination was produced in rat sciatic nerve by unilateral intraneural injection of anti-galactocerebroside serum. A functional lesion was confirmed by the presence of nerve conduction block. Histologically, this corresponded to demyelination of 50–70% of the fibers in nerve cross sections; axonal structures appeared intact.

At the time of maximal demyelination (7 d), ^{35}S-methionine or ^{3}H-fucose was injected bilaterally into the spinal cord ventral horn. At later times (5 hr–7 d), the sciatic nerve was removed and radioactivity in successive nerve segments was quantitated. The transport rates (~260 mm/d) and the composition of transported proteins and glycoproteins (separated on 7–15% polyacrylamide gradient gels) were not altered in lesioned nerves relative to contralateral control nerves.

Light microscopic autoradiographic analysis revealed a similar localization of axonally transported and deposited glycoproteins in demyelinated and control fibers. Initially (8 hr), the majority of label was over axons. Labeled glycoproteins remaining in the nerve after 1 week were retained mainly in axolemmal regions.

We conclude that acute focal primary demyelination does not lead to major alterations in the transport or deposition of newly synthesized macromolecules.

Myelin, segments of lipid-enriched glial cell membrane wrapped around axons, is required for normal saltatory conduction of electrical impulses along axons (for review, see Ritchie, 1984a). Thus, demyelination, characteristic of a number of disease and toxic states (for reviews, see Morell et al., 1981; Traugott and Raine, 1984), leads to blocked impulse conduction along axons and therefore impaired neurotransmission (see review by Ritchie, 1984b). However, the interaction between axons and their ensheathing myelin extends beyond facilitation of impulse conduction. As was described by Ramón y Cajal (1928), when an axon is lesioned both the axon and myelin degenerate. The converse situation, the effect of primary demyelination on the neuron, is less clear. Primary demyelination has been associated with axonal caliber reduction (for discussion, see Prineas and McLeod, 1976; Aguayo et al., 1979) and axolemmal remodeling (Ritchie et al., 1981).

We have chosen to study neuronal metabolic responses to myelin loss by examining axonal transport. In neurons, macromolecules are synthesized in the cell body and must be transported along axons to be utilized in maintenance of axonal components and for continuation of synaptic function (for reviews, see Grafstein and Forman, 1980; Ochs, 1982; Weiss, 1982). Correlative biochemical and autoradiographic analysis of axonal transport enabled us to search for general metabolic perturbations of the cell, as well as for alterations restricted to the demyelinated region.

We hypothesized 3 possible results of acute focal demyelination with respect to general or local changes in rapid axonal transport. First, transport could be impaired, indicating that axonal damage may be occurring secondary to the primary demyelination. Second, axonal transport might be enhanced. This might happen, for example, if the denuded region of the axon required an increased supply of macromolecules to compensate for demyelination as a means of preventing neuronal degeneration and/or promoting remyelination. Third, within the sensitivity of the analytical techniques utilized, axonal transport could be unchanged, suggesting that the focally demyelinated axons are able to continue some normal metabolic functions. This might implicate additional pathologic factors, other than simply the absence of myelin, as causes of axonal damage when axonal degeneration is associated with primary demyelination. In this study we attempted to distinguish among these possibilities in order to better understand the pathophysiology of demyelination.

Materials and Methods

Experimental design. The general protocol used in this study is outlined in Figure 1. Demyelination was initiated in one sciatic nerve of each rat by intraneural injection of anti-GC sera. Only those rats exhibiting a functional correlate of demyelination (i.e., nerve conduction block along the lesioned nerve 3–4 d after injection of anti-GC sera, see below for criterion) were included in subsequent studies. During the time period corresponding to maximal demyelination (7 d after anti-GC sera; see Saida et al., 1979, 1980), ^{35}S-methionine was injected into the spinal cord ventral horn to label transported proteins. In a separate series of animals, ^{3}H-fucose was used for specifically labeling glycoproteins. At various time intervals between 5 hr and 7 d following precursor injection, rats were sacrificed for either biochemical or autoradiographic analysis.

Animals. Male Long-Evans hooded rats (Charles River Laboratories, Wilmington, MA), approximately 4 months of age, were used throughout the study. Anesthesia was induced by intramuscular forelimb injection of ketamine (37 mg/kg; Parke-Davis, Morris Plains, NJ) and xylazine (9 mg/kg; Miles Laboratories, Shawnee, KS), with a subcutaneous atropine pretreatment (1.0 cc/rat; Elkins-Sinn, Cherry Hill, NJ) to inhibit bronchial secretions.

Received Mar. 13, 1987; revised June 3, 1987; accepted June 3, 1987.

We wish to thank James F. Howard Jr., M.D., for assistance in the nerve conduction studies, Dr. Robert M. Gould for sharing autoradiography and intraneural injection techniques, and John W. Griffin, M.D., for demonstrating the method of precursor injection. We are also grateful to Steve Levison for performing immunocytochemical staining and to Steve Peck and Matt Koch for carrying out the statistical analyses. This research was supported by USPHS Grants NS11615, ES01104, and HD03110. R.A. was a NSF predoctoral fellow.

Correspondence should be addressed to Dr. Pierre Morell, 321 Biological Science Research Center 220H, University of North Carolina, Chapel Hill, NC 27514.

Copyright © 1987 Society for Neuroscience 0270-6474/87/124044-12$02.00/0

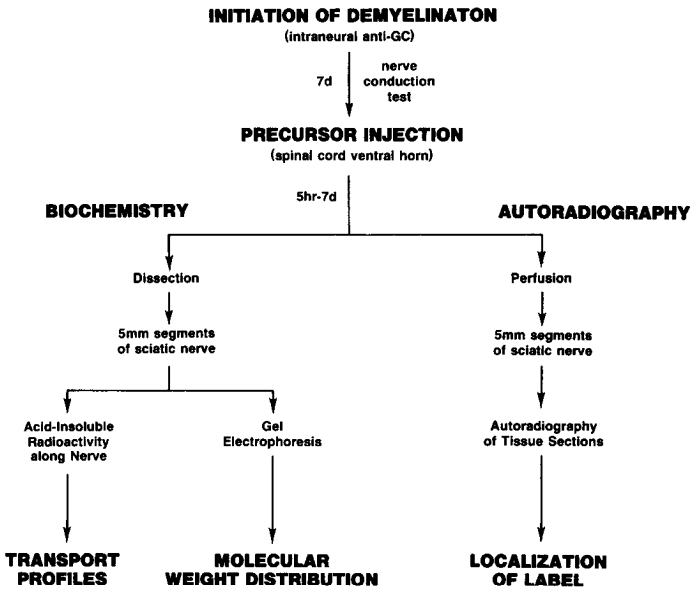

Figure 1. Experimental design.

Induction of demyelination. The polyclonal antisera to GC (anti-GC sera) used in this study were the generous gifts of Dr. Joyce Benjamins and Dr. Donald Silberberg. The sera were prepared by inoculating rabbits with an emulsion of GC and either keyhole limpet hemocyanin (Benjamins et al., 1986) or ovalbumin (Hirayama et al., 1984).

Anti-GC sera titers were assayed by antisera precipitation of GC-containing liposomes labeled with ^{3}H-cholesterol (Fry et al., 1976). Both sera demonstrated specificity for GC at titers considered relatively high in this assay system (Benjamins, 1:256; Silberberg, 1:128). The specificity of the antisera was also tested by immunocytochemical staining of cultured process-bearing cells (oligodendrocytes) following methods described by Trimmer and McCarthy (1986). The polyclonal anti-GC sera consistently stained coincident with a monoclonal anti-GC serum (data not shown).

Intraneural injection techniques described by Hall and Gregson (1971) and Saida and co-workers (1978, 1979) were modified to minimize injection trauma (Dyck et al., 1982; Hughes et al., 1985). Briefly, while rats were under anesthesia, the right sciatic nerve was exposed in the upper thigh region without disrupting the blood supply to the nerve. Countertraction on the nerve was applied lightly with a smooth glass hook while a fine-tipped glass micropipette was inserted under the perineurium with the aid of a micromanipulator. Twenty-five microliters of anti-GC serum was slowly injected using gentle back-pressure from an air-filled syringe. The injection site was marked by a 5-0 silk ligature in the subjacent musculature. Possible nonspecific effects from injection trauma and sera constituents were examined in a series of animals injected intraneurally with 25 μl of normal rabbit serum.

Nerve conduction studies. Our nerve conduction studies were based on methods of Sumner and colleagues (1982). Rats were anesthetized and placed on 37°C isothermal heating pads (Deltaphase pads; Braintree Scientific, Braintree, MA). Steel monopolar stimulating electrodes were inserted percutaneously (Fig. 2) at the hip (close to the nerve at the sciatic notch, S_1) or at the ankle (adjacent to the posterior tibial nerve branch, S_2). The active recording electrode (R) just penetrated the dorsal surface of the hind foot, and the reference recording electrode was positioned in the tendon on the lateral foot surface. A ground electrode was placed in the lower thigh.

Compound muscle action potentials evoked by supramaximal 0.1 msec square-wave stimulus pulses were amplified and displayed on a TECA TE42 electromyograph. The amplitudes (baseline to negative peak) and latencies (stimulus to onset of response) were measured for the M- and F-waves of each potential (see inset of Fig. 2). The distance between the hip (S_1) and ankle (S_2) stimulating sites was measured with the hindlimb fully extended.

Since the amplitude of a compound potential reflects the number of stimulated fibers conducting impulses to the recording site, a ratio of the hip (S_1) amplitude to the ankle (S_2) amplitude was used to estimate the proportion of fibers conducting through the demyelinated region.

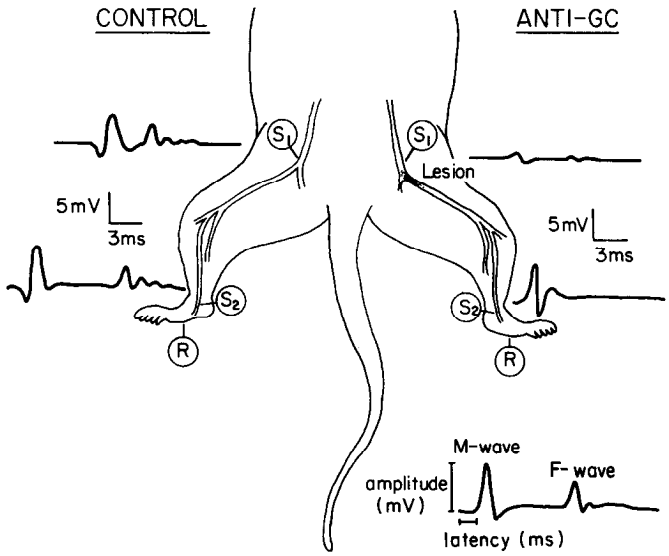

Figure 2. Schematic diagram of a rat hindquarters indicating the positioning of the stimulating electrodes (S_1 and S_2) and the active recording electrode (R) in relation to the sciatic nerve. The *lower-right inset* identifies the relevant features of a typical compound muscle action potential (M-wave) and the late response, F-wave. An M-wave arises from impulses traveling directly from the point of nerve stimulation to the recording site in the foot. An F-wave arises from impulses traveling antidromically, from the point of nerve stimulation to the cell bodies in the spinal cord, and then orthodromically to the recording site in the foot. The amplitude of the compound muscle action potential was taken as the maximal negative voltage difference of the M-wave above the baseline. The latency is measured from the time of stimulation until the onset of a response.

Insets adjacent to each stimulation site show an example of traces from impulses originating at each of the 4 stimulation sites in a single animal. Note the diminished amplitudes of compound potentials arising from impulses that travel through the demyelinated region to reach the recording site (M-wave and F-wave from stimulation at S_1, *upper-right tracing*; F-wave from stimulation at S_2, *lower-right tracing*).

Conduction block was defined as a reduction in the S_1:S_2 amplitude ratio of more than 2 SD below control values (control M-ratio = 0.91 ± 0.13, based on recordings from noninjected nerves of a preliminary set of 9 control animals). Conduction velocity was calculated as the distance between stimulating sites divided by the latency difference between hip and ankle stimulation.

Injection of radiolabeled precursor. Precursor injection was restricted to rats exhibiting extensive demyelination, as determined by the presence of nerve conduction block. Seven days after intraneural injection of anti-GC sera (the time corresponding to maximal demyelination, see Saida et al., 1979, 1980), animals were placed under anesthesia, and a dorsal laminectomy was performed to expose the lower thoracic and upper lumbar spinal cord. As described by Griffin and coworkers (1976), the insertion site of the L5 dorsal roots into the spinal cord was identified, and a small puncture was created in the dura over the right crown of the spinal cord at that level. A fine-tipped glass micropipette containing radiolabeled precursor was secured in a micromanipulator and lowered 1.5 mm down through the dural opening into the spinal cord ventral horn region (vicinity of sciatic nerve motor neuron cell bodies). Radioisotope (400 μCi in 1 μl sterile normal saline) was slowly injected using gentle back-pressure from an air-filled syringe. The radiolabeled precursor was either L-^{35}S-methionine (1120 Ci/mmol; New England Nuclear, Boston) or L-5,6-^{3}H-fucose (60 Ci/mmol; ARC, St. Louis). This injection procedure was repeated on the left side of the spinal cord. The surgical field was flushed with sterile normal saline prior to closure of the incision with metal wound clips. During recovery, each animal was placed on a 37°C isothermal heating pad to maintain its body temperature.

Biochemical analysis. Rats were sacrificed by exposure to ether at

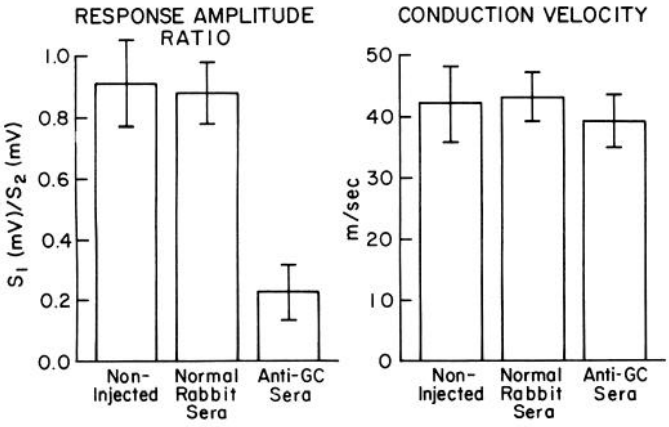

Figure 3. Nerve conduction study data. The ratio of the M-wave response amplitude from stimulation at S_1 versus S_2 is significantly decreased in anti-GC injected nerves, indicating a decrease in the number of fibers that were able to conduct impulses through the demyelinated region. The conduction velocity is not slowed in lesioned nerves, which indicates that at least some of the fastest conducting fibers are not demyelinated. Values for anti-GC lesioned nerves include only rats subsequently used for biochemical or autoradiographic analysis (n = 19); noninjected nerves (n = 23) are contralateral to nerves injected with either anti-GC sera (n = 19) or normal rabbit sera (n = 4). Values are means ± SEM.

times ranging from 5 hr to 7 d after precursor injection. On both sides of the animals, the spinal cord precursor injection site, L4 and L5 spinal roots, and sciatic nerve and branches were dissected and sectioned into sequential 5 mm segments along the length of the roots and nerves. Tissue samples were freeze-dried, partially delipidated with ether : ethanol (3:2), and dried under nitrogen (Morell et al., 1975). Each segment was then solubilized in 100 μl of 1% SDS with the aid of a sonicating bath. Aliquots were removed to determine the protein content (Lowry et al., 1951), the total radioactivity, and the acid-soluble and acid-insoluble radioactivity (Goodrum et al., 1979). The remainder of each solubilized segment was subjected to electrophoresis, using discontinuous polyacrylamide gradient gels (3% stacking gel; 7–15% gradient running gel) in buffers containing SDS (Maizel, 1971; Padilla et al., 1979). Proteins labeled with ^{35}S-methionine were separated on slab gels (180 × 130 × 1 mm); the molecular-weight distribution of labeled proteins was visualized with Kodak X-Omat AR film and analyzed with a Zeineh model SL-504-XL soft laser scanning densitometer (Biomed Instruments, Inc., Fullerton, CA). Glycoproteins, labeled with ^{3}H-fucose, were separated on cylindrical gels (6 × 150 mm) to facilitate quantitation of the lower-energy tritium label. Gels were sliced into 1.1 mm segments with a Hoefer gel slicer, and the radioactivity in each slice determined by liquid scintillation counting (Goodrum et al., 1979; Toews et al., 1982).

Statistical analysis. The nerve conduction data (M-ratios and conduction velocities) for anti-GC lesioned nerves were compared with data recorded from the contralateral control nerves by a paired t test analysis.

The maximal transport rate was calculated from the displacement of the front of radioactivity down the nerve with time. The transport rate was taken as the slope of the best straight line through the points, as fit by linear regression. Possible differences between the slopes in demyelinated and contralateral control nerves were examined using a paired data version of the t test.

Transport profiles (distribution of radioactivity along each nerve) were analyzed to test the significance of local variations in the levels of radioactivity in demyelinated regions. Since label was equilibrated along the nerves at 1 d and 1 week after precursor injection, the transport profiles should approximate a straight line. Therefore, the best line through the points 50–110 mm from the precursor injection site was fit by linear regression for each nerve. Along focally demyelinated nerves, the 2 points in the demyelinated region were excluded from the straight line estimates. The variation of these 2 values from the predicted best straight line along the nerve was then tested for significance with an F test.

Autoradiographic localization of labeled glycoproteins. Eight hours, 1 d, or 1 week after bilateral intracord injection of ^{3}H-fucose, each rat was anesthetized and the sciatic nerves on both sides exposed at the thigh and fixed *in situ* for an hour with 4% glutaraldehyde in 0.1 M cacodylate buffer (Morris et al., 1972). Rats were then sacrificed and the anti-GC lesion sites and corresponding contralateral control segments of sciatic nerve (75–80 mm from the ^{3}H-fucose injection sites)

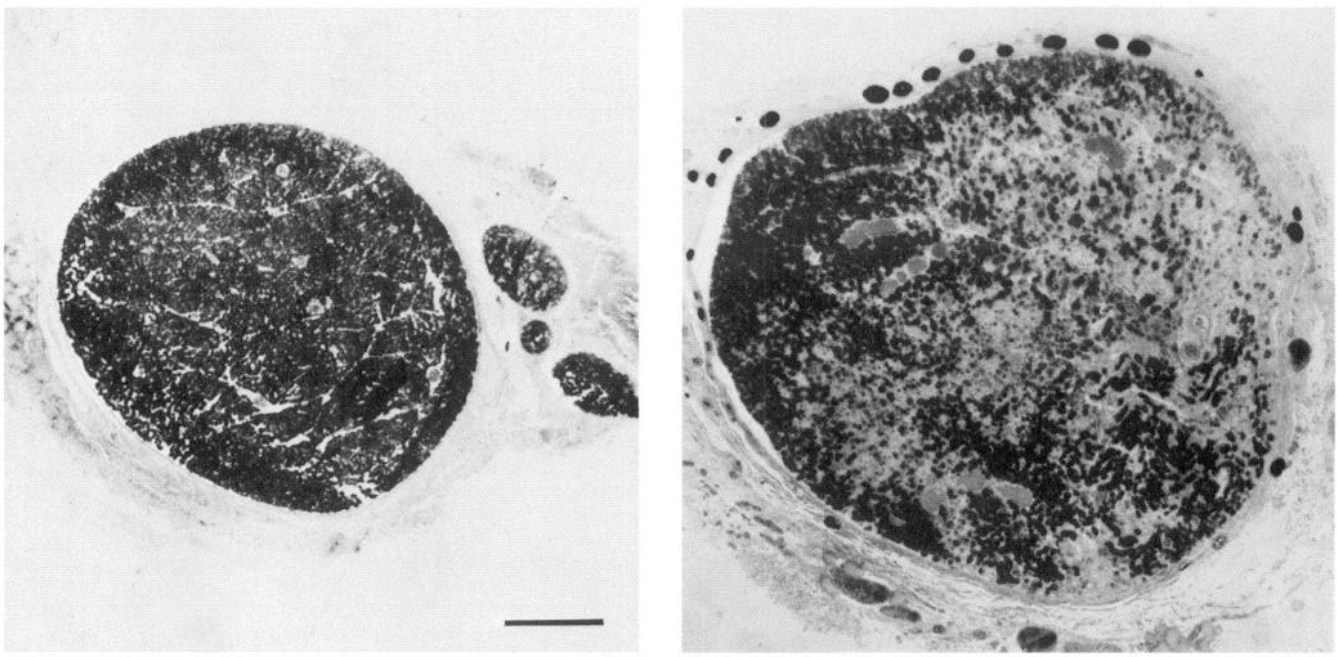

Figure 4. Cross sections of demyelinated and contralateral control sciatic nerves at 7 d after anti-GC sera injection. In control tissue (*left panel*) myelin is darkly stained over the entire fascicle. At the site of anti-GC lesion (*right panel*), extensive demyelination is evident over the large portion of the fascicle which has lost the dark myelin stain. The increased overall size of the lesioned fascicle is due to hypercellularity related to the immune-mediated response. Toluidine blue. Scale bar, 0.2 mm.

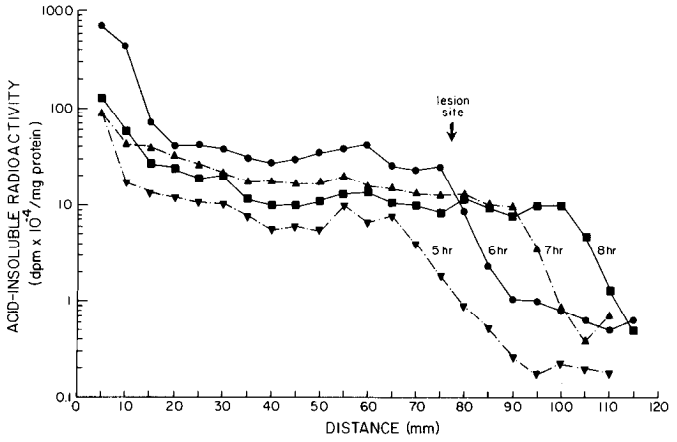

Figure 5. Distribution of axonally transported labeled proteins along anti-GC lesioned nerves at various times after [^{35}S]methionine injection. The front of transported label is displaced along the nerve with time. 5 hr (▼); 6 hr (●); 7 hr (▶); 8 hr (■).

were excised. Nerve segments were stored in fixative overnight, washed in buffer for several days, postfixed with 1% osmium tetroxide for 2 hr, dehydrated in graded alcohols, cleared with propylene oxide, and embedded in Spurr's resin (Bouldin and Cavanagh, 1979). Transverse sections (0.5 μm) on gelatin-chrome alum-coated slides were dipped in Kodak NTB2 nuclear track emulsion, exposed at 4°C for 49 d, developed at 16°C in Kodak D19, and stained with toluidine blue (Williams, 1977).

Light microscopic photographs (2000×) of tissue cross sections were analyzed with a Zeiss Videoplan Image Analysis System using software version 4.3 (Carl Zeiss, Inc., Thornwood, NY). Silver grains (which indicate the presence of labeled glycoproteins) were counted over the following morphologic compartments: axons, axolemmal regions, myelin, phagocytic cells and debris, and remyelinating ensheathing cells. Simultaneously, the area of each compartment was measured on the digitizer tablet interfaced with the Videoplan. The grain density for each compartment was calculated as the number of grains over the compartment divided by the area of the compartment.

Results

Confirmation of demyelination

Three or 4 d after anti-GC sera injection into the sciatic nerve, a functional correlate of extensive demyelination was confirmed by the presence of impulse conduction block along the lesioned sciatic nerve. Actual traces from one animal are shown in Figure 2.

The mean of the M-wave amplitude ratios (Fig. 3) was 0.91 ± 0.15 in noninjected nerves (n = 23) and 0.88 ± 0.10 in nerves injected with normal rabbit serum (n = 4). In contrast, the mean ratio was 0.22 ± 0.10 in anti-GC lesioned nerves of rats subsequently used for biochemical or autoradiographic analysis (n = 19). The lesioned nerve values are significantly lower ($p < 0.001$) than the values for the contralateral control nerves, indicating impairment of impulse conduction. The impaired conduction does not result from injection trauma since conduction is not disrupted in nerves injected with normal rabbit serum. The nerve conduction velocity (Fig. 3; noninjected = 43.8 ± 6.5 m/sec; normal rabbit sera injected = 43.1 ± 4.0 m/sec; anti-GC sera injected = 40.3 ± 5.5 m/sec) was not slowed significantly in lesioned nerves ($p > 0.05$), indicating that at least some of the fastest conducting fibers were not demyelinated. Our values are similar to those reported by Sumner and coworkers (1982) for this same model of focal demyelination.

It has been previously shown (Sumner et al., 1982) that nerves exhibiting conduction block go on to demyelinate extensively

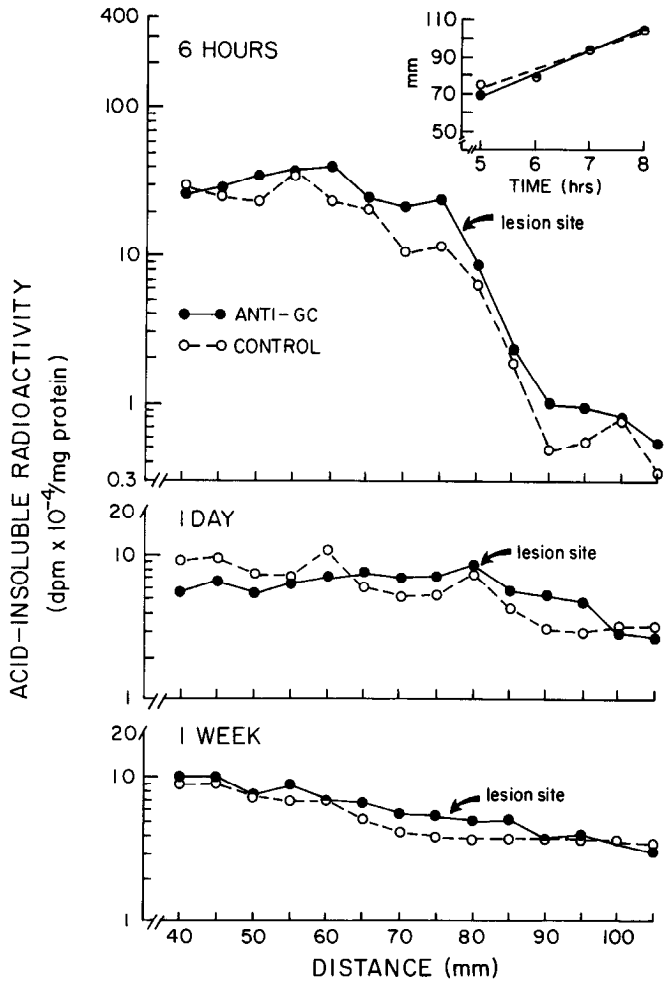

Figure 6. Comparison of the distribution of ^{35}S-methionine-labeled proteins in anti-GC lesioned and contralateral control nerves at 6 hr, 1 d, or 1 week after precursor injection. Each panel compares sequential 5 mm segments along the nerves from opposite sides of the same animal. The *inset* shows the positions of the front of transported radioactivity in lesioned and control nerves plotted against the length of time between precursor injection and sacrifice. The transport rates for control nerves (252 mm/d) and lesioned nerves (288 mm/d) were determined from the slope of the best straight line through these points, as fit by linear regression.

within 7 d following anti-GC sera injection. Our histologic examination (Fig. 4) of 3 antisera injected nerves exhibiting nerve conduction block confirmed the presence of widespread demyelination in each of the nerves. At the site of anti-GC sera injection, demyelination was evident across 50–70% of the area in cross sections (areas calculated from digitized outlines of the demyelinated regions in micrographs enlarged 75×). Longitudinal sections of adjacent nerve segments revealed demyelination extending approximately 0.5–1.0 cm proximally and/or distally from the antisera injection site.

Axonal transport profiles

^{35}S-methionine-labeled proteins. Following injection of ^{35}S-methionine into the vicinity of the sciatic motor neuron cell bodies, radioactive label was incorporated into newly synthesized proteins, some of which were subsequently committed to axonal transport. Labeled proteins were transported down the axons

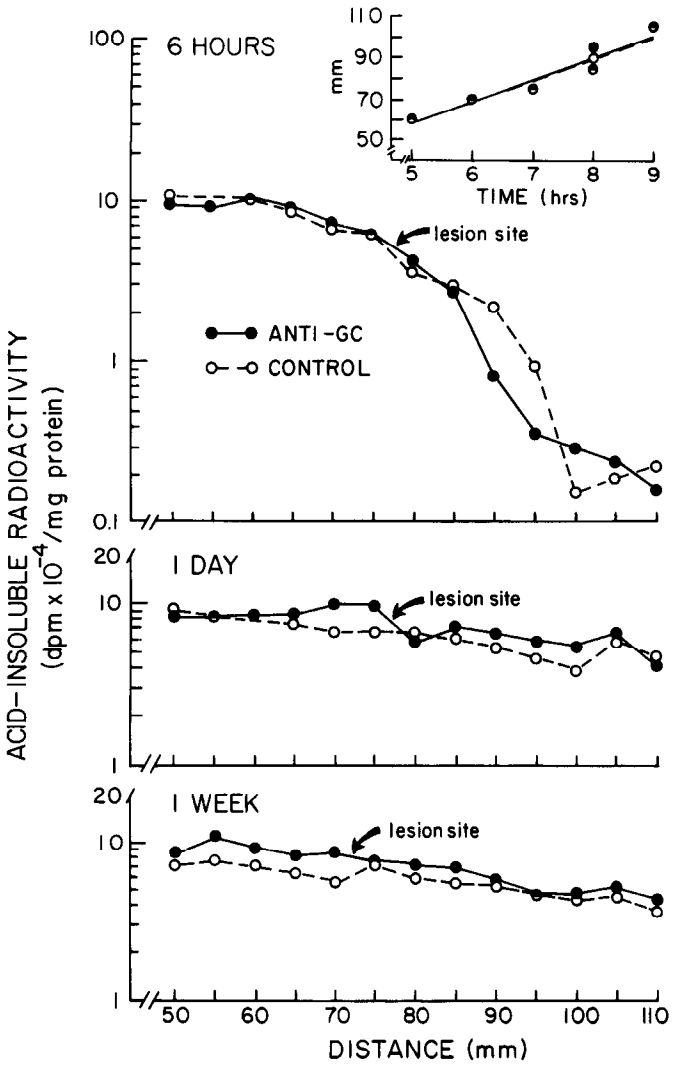

Figure 7. Comparison of the distribution of ^{3}H-fucose-labeled glycoproteins in anti-GC lesioned and contralateral control nerves at 6 hr, 1 d, or 1 week after precursor injection. The transport rates for control (252 mm/d) and lesioned (261 mm/d) nerves were determined as described in Figure 6.

as a front of radioactivity followed by a relatively flat plateau (Fig. 5).

Possible effects of demyelination on axonal transport of proteins were examined by a within-animal comparison of transport profiles for the anti-GC lesioned nerve and contralateral control nerve (Fig. 6). At early times following precursor injection (Fig. 6, upper panel), the shape of the transport profiles were very similar for lesioned and control nerves. The maximal rates of protein transport, calculated from the rate of displacement of the radioactive front (Fig. 6, inset in upper panel), were not significantly different (control = 252 mm/d; lesioned = 288 mm/d; $p = 0.22$) and are consistent with rapid anterograde transport rates reported in this and other systems (for review, see Grafstein and Forman, 1980). Although the initial front of transported radioactivity passes through the region of focal demyelination (75–80 mm from the spinal cord) approximately 7 hr after precursor injection, displacement of the front down the nerve was linear between 5 and 8 hr. Therefore, it is unlikely that the fastest moving proteins were slowed locally in the demyelinated region.

With increasing time after precursor injection, the front of ^{35}S-methionine-labeled proteins travels the length of the nerve. At 1 d (Fig. 6, middle panel), the transport profiles show the flattened plateau region extending to the most distal segments. Profiles from lesioned and control nerves were similar, although the level of radioactivity was consistently slightly higher in the demyelinated region of the lesioned nerves (for nerve in Fig. 6 at 75 mm, $p = 0.18$; at 80 mm, $p = 0.04$).

The radioactivity present in the nerve 1 week after precursor injection (Fig. 6, lower panel) is mostly from labeled molecules that have been carried in the rapid transport phase and deposited along the axons, and from labeled molecules moving at intermediate transport rates. The profiles for lesioned and control nerves were similar. Label was not increased in the region of focal demyelination relative to other regions of the nerve (for the nerve in Fig. 6 at 75 mm, $p = 0.77$; at 80 mm, $p = 0.77$).

^{3}H-fucose-labeled glycoproteins. Glycoproteins undergo rapid anterograde transport and some transported glycoproteins are deposited in axolemmal membranes (Griffin et al., 1981; Goodrum and Morell, 1982; Toews et al., 1982). Thus, alterations in the axonal transport and deposition of these macromolecules might follow metabolic insult to the axolemma.

Profiles of ^{3}H-fucose-labeled glycoproteins at early times following labeling (Fig. 7, upper panel) had a less distinct front than ^{35}S-methionine-labeled proteins (Fig. 6, upper panel), as has been previously noted by others (Stromska et al., 1981). More importantly, the patterns of ^{3}H-fucose label (wavefront and plateau) were similar along lesioned and control nerves. The maximal rate of glycoprotein transport (Fig. 7, upper panel inset) was similar along lesioned and control nerves (261 and 252 mm/d, respectively; $p = 0.59$). These rates are consistent with the rate of rapid anterograde transport of glycoproteins reported in sciatic nerve sensory neurons (Toews et al., 1982) and in other systems (for review, see Elam, 1979). Also, the linear displacement of the labeled front during its movement along the focally lesioned nerves indicates that local slowing of the fastest moving glycoproteins is unlikely.

With longer time intervals, the ^{3}H-fucose-labeled glycoproteins become distributed along the entire nerve. Transport profiles 1 d after precursor injection (Fig. 7, middle panel) were similar for lesioned and control nerves. Profiles of radioactivity deposited over 1 week along the lesioned and control nerves were also similar (Fig. 7, lower panel). In the region of demyelination the increase in deposition of labeled glycoproteins at 1 d and 1 week did not reach statistical significance (for nerves shown in Fig. 7; 1 d at 70 mm, $p = 0.15$; 1 d at 75 mm, $p = 0.08$; 1 week at 75 mm, $p = 0.33$; 1 week at 80 mm, $p = 0.52$).

Molecular-weight distribution of transported macromolecules

In order to determine whether demyelination alters the composition of axonally transported material, the molecular-weight distributions of labeled proteins and glycoproteins present in the demyelinated segments were compared with those of contralateral control segments.

The ^{35}S-methionine-labeled proteins separated into several major bands on 7–15% polyacrylamide slab gels (Fig. 8). At an early transport time (8 hr), when the moving front has just passed through the sampled segment, labeled bands corresponding to apparent molecular weights of approximately 112, 93, 23, and 21 kDa were prominent in both the demyelinated and control segments. With increasing time after precursor injection (1 d, 1 week), proteins in the 57–44 kDa range represented a

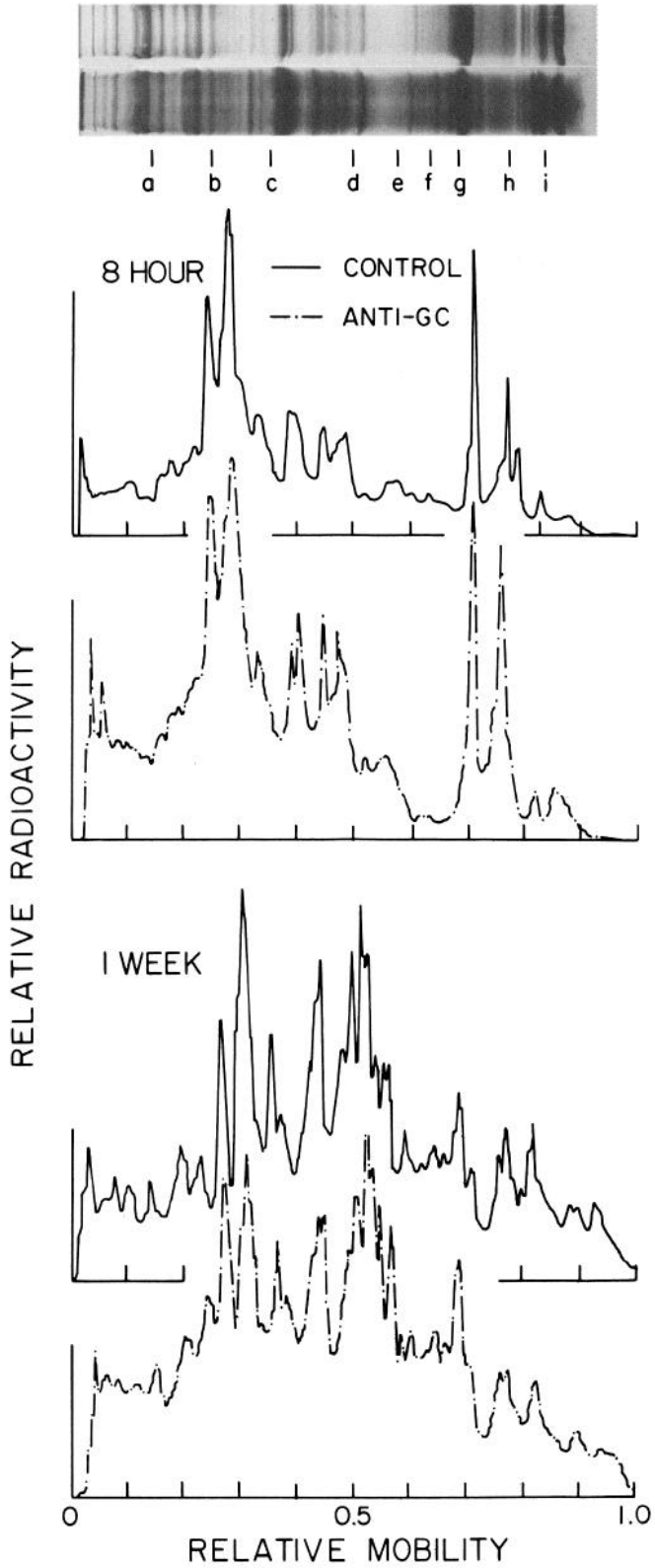

Figure 8. Gel electrophoretic distribution of ^{35}S-methionine-labeled proteins in sciatic nerve (anti-GC site and contralateral control segment). Proteins were separated on 7–15% polyacrylamide gradient slab gels; the molecular-weight distribution of labeled proteins was visualized with x-ray film and analyzed by scanning laser densitometry. Data are plotted as relative radioactivity (optical density of the autoradiogram, with the scanning sensitivity adjusted to give 85% of full response for the densest band of each sample) versus relative mobility (marker dye front = 1.0). The aliquot of sample applied to each gel lane contained approximately 36,000 dpm for the 8 hr control segment and 47,000 dpm for the 8 hr demyelinated segment, while the 1 week segments contained approximately 18,000 and 25,500 dpm, respectively. *Inset,* Typical Fast green staining patterns of a control segment (*upper lanes*) and lesioned site (*lower lanes*). The average positions of the *M,* standards are indicated (*a,* myosin 205 kDa; *b,* β-galactosidase 116 kDa; *c,* bovine albumin 66 kDa; *d,* ovalbumin 45 kDa; *e,* glyceraldehyde-3-phosphate dehydrogenase 36 kDa subunit; *f,* carbonic anhydrase 29 kDa; *g,* trypsinogen 24 kDa; *h,* trypsin inhibitor 20.1 kDa; *i,* α-lactalbumin 14 kDa).

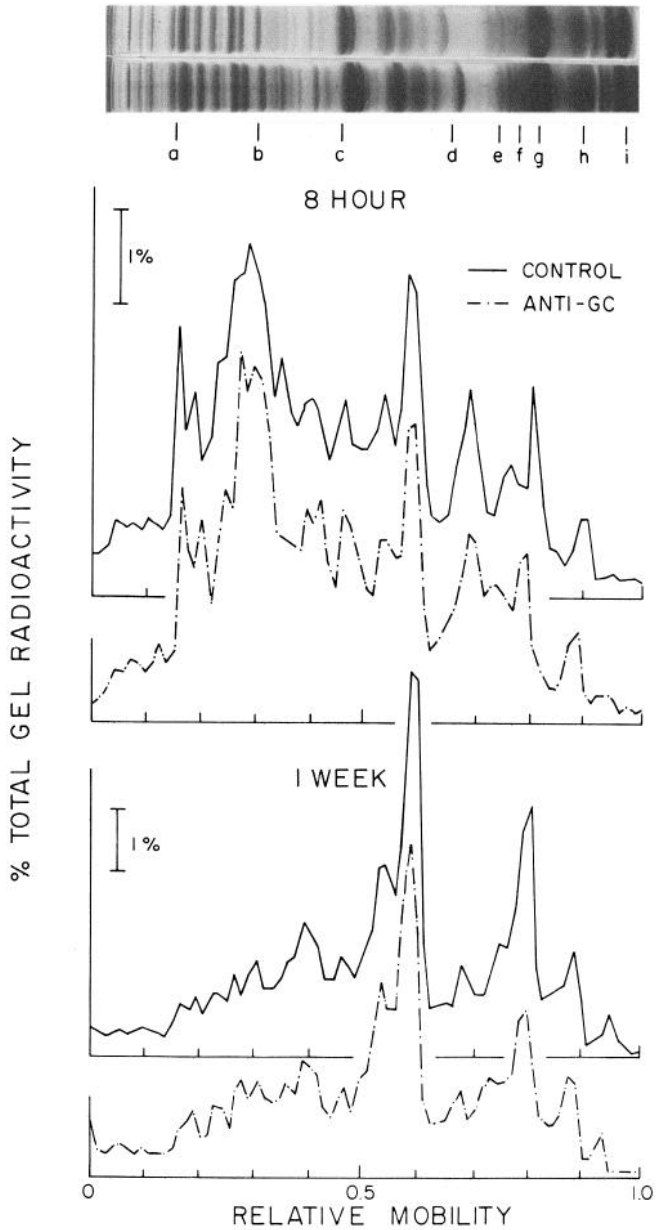

Figure 9. Gel electrophoretic distribution of ^{3}H-fucose-labeled glycoproteins in sciatic nerve (anti-GC site and contralateral control segment). Glycoproteins were separated on 7–15% polyacrylamide gradient cylindrical gels and the radioactivity present in 1.1 mm slices of the gels determined by liquid scintillation counting. The aliquot of sample applied to each gel contained approximately 36,000 dpm for the 8 hr control segment and 33,500 dpm for the 8 hr demyelinated segment, while the 1 week segments contained approximately 30,000 and 40,000 dpm, respectively. *Inset,* Typical Fast green staining patterns and the average positions of the *M,* standards (see Fig. 8).

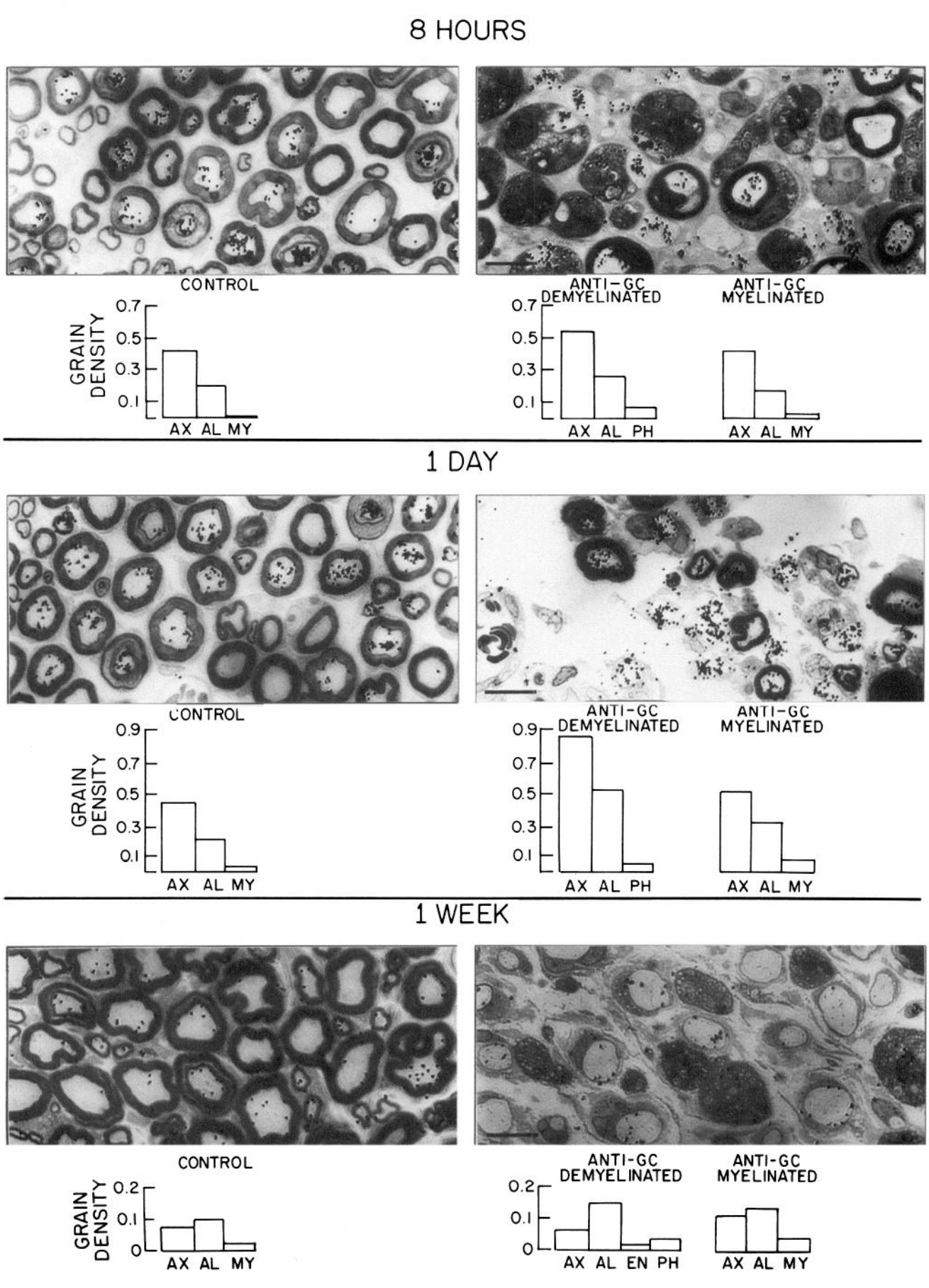
8 HOURS
CONTROL
ANTI-GC DEMYELINATED
ANTI-GC MYELINATED
GRAIN DENSITY
0.7
0.5
0.3
0.1
AX AL MY
AX AL PH
AX AL MY
1 DAY
CONTROL
ANTI-GC DEMYELINATED
ANTI-GC MYELINATED
GRAIN DENSITY
0.9
0.7
0.5
0.3
0.1
AX AL MY
AX AL PH
AX AL MY
1 WEEK
CONTROL
ANTI-GC DEMYELINATED
ANTI-GC MYELINATED
GRAIN DENSITY
0.2
0.1
0
AX AL MY
AX AL EN PH
AX AL MY

relatively greater proportion of the total label present, while those of lower molecular weight were relatively decreased. This shift in the relative molecular-weight distribution with time is likely to result from deposition of labeled molecules (Ochs, 1975; Munoz-Martinez et al., 1981) and from the appearance of different labeled proteins moving at an intermediate transport rate (Willard et al., 1974; Padilla et al., 1979; Toews et al., 1982). No marked differences were observed between the molecular-weight distributions of ^{35}S-methionine-labeled proteins in demyelinated and contralateral control segments at 8 hr, 1 d, or 1 week. In addition, demyelinated segments were not notably different from segments proximal and distal to the lesioned area (data not shown).

The ^{3}H-fucose-labeled glycoproteins were separated on 7–15% polyacrylamide gradient cylindrical gels (Fig. 9). At the earliest transport time examined (8 hr), a complex pattern of label distribution was present in both demyelinated and control nerve segments. The most prominent labeled peaks correspond to approximately 132, 118, and 49 kDa molecular weights. By 1 week after precursor injection, the higher molecular weight bands had decreased in prominence relative to the 49 kDa peak, and a band near 25 kDa was relatively well labeled. The majority of radioactivity observed at this time presumably represents labeled glycoproteins that have been deposited along the axons in addition to glycoproteins labeled by reutilization of the labeled fucose moiety from axonally transported glycoproteins previously deposited (Goodrum and Morell, 1982; Toews et al., 1982). There were no marked differences in the molecular-weight distribution of labeled glycoproteins specific to the demyelinated segments compared to either contralateral control tissue or segments proximal and distal to the lesioned area.

Autoradiographic localization of transported glycoproteins

Light microscopic autoradiography was used to visualize the location of axonally transported glycoproteins (Fig. 10). The moving front of ^{3}H-fucose-labeled molecules is just past the sampled tissue segment (75–80 mm from the spinal cord) at the 8 hr transport time. At this time (Fig. 10, upper panel), the silver grains (which indicate labeled glycoproteins) are located mainly over axons, with very few present over axolemmal regions or myelin. The distribution was the same over myelinated and demyelinated fibers. One day after precursor injection (Fig. 10, middle panel), label is still mostly over axons in both myelinated and demyelinated fibers. The grain density over demyelinated fibers is increased relative to myelinated fibers, but this is at least partially due to a transient decrease in fiber size that accompanies demyelination (Saida et al., 1979, 1980). The grain distribution is shifted by 1 week (Fig. 10, lower panel); the densest labeling is now over the axolemmal region, as has also been observed in normal tissue by Griffin and coworkers (1981). This deposition of label is approximately equivalent in myelinated and demyelinated fibers. These autoradiographic data indicate that there is not a marked differential deposition or transfer of axonally transported glycoproteins in demyelinated fibers.

Discussion

We have reproduced a previously established model of focal primary demyelination in order to characterize the effects of demyelination with respect to axonal transport. Intraneural injection of anti-GC sera in rat sciatic nerve has been previously shown to result in antibody-dependent, complement-mediated lysis of myelin followed by phagocytosis (Saida et al., 1979). With high-titer antisera, nerve conduction block is present within 1 d and extensive demyelination follows (Sumner et al., 1982). The majority of axons in a cross section of nerve become denuded between 5 and 7 d (Saida et al., 1979; Hughes et al., 1985), while remyelination begins within 8–10 d of antisera injection (Saida et al., 1980).

Using this localized, myelin-specific model of demyelination, we have found that the distribution of axonally transported proteins and glycoproteins along nerves at various transport times was not altered appreciably in demyelinated nerves relative to control nerves. Thus, the maximal transport rate did not vary, and the amount of radioactivity in transport or deposited was always similar between the demyelinated nerve and contralateral control nerve of the same animal. Examination of the molecular-weight distribution of labeled proteins and glycoproteins also did not reveal any marked qualitative or quantitative differences between demyelinated and control nerve segments.

While most axonally transported glycoproteins are targeted to nerve endings, some are deposited in axolemmal membranes (Griffin et al., 1981; Goodrum and Morell, 1982; Toews et al., 1982). Thus, effects associated with demyelination (e.g., remodeling of the nodal membrane, see Ritchie et al., 1981), which involve molecules known to be glycoproteins (e.g., sodium channels, see Catterall, 1984), might correspond to changes in the axonal transport and deposition of glycoproteins. Quantitative autoradiography of labeled axonally transported glycoproteins demonstrated that, with time, label was deposited in the axolemmal region. However, the time course and extent of deposition was similar in both demyelinated and myelinated fibers.

Our biochemical and autoradiographic data indicate that rapid anterograde axonal transport of proteins and glycoproteins is not affected by focal disruption of myelin with anti-GC sera. Consistent with this interpretation is data, presented in abstract form (Parhad et al., 1982; Parhad and Griffin, 1986), concerning an autoradiographic analysis of fucosylated glycoprotein transport and deposition in rat sciatic nerve focally demyelinated by exposure to lysolecithin solution. In apparent contradiction is a report of accumulation of rapidly transported proteins in regions of chicken sciatic nerve demyelinated with diptheria toxin (Kidman et al., 1978a, b). The discrepancy may arise from species differences or varied extents of demyelination; however, it is difficult to dismiss axonal damage as a cause of the accumulation of transported material. In studies utilizing models of systemically induced demyelination, alterations of the rapid transport of proteins have been reported (Rao et al., 1981; Pes-

←

Figure 10. Autoradiographic localization of ^{3}H-fucose-labeled glycoproteins in sciatic nerve cross sections of the anti-GC lesion site and the contralateral control segment (each 75–80 mm from the spinal cord). Seven days after demyelination was initiated, precursor was injected into the spinal cord. Rats were sacrificed 8 hr, 1 d, or 1 week later and the tissue processed for light microscopic autoradiography.

Grain densities are calculated from the number of grains over a structural compartment divided by the area of the compartment. Histograms of the grain densities correspond to the above micrographs (*left*, control; *right*, anti-GC). Within the anti-GC tissue, demyelinated and myelinated fibers were quantitated separately. *AX*, axon; *AL*, axolemmal region; *MY*, myelin; *PH*, phagocytic cells and debris; *EN*, remyelinating ensheathing cells. Scale bar, 0.01 mm.

soa and Ikeda, 1984; Tansey and Ikeda, 1986). The relevance of these data to studies of demyelination-induced alterations in axonal transport is equivocal. The systemic nature of the pathology creates difficulty in verifying that there are not associated axonal or neuronal lesions, and thus effects specific to demyelination cannot be identified with certainty. We suggest that previously reported alterations of rapid axonal transport during demyelination may, in fact, reflect damage to neurons and that sufficiently specific focal demyelination has only minimal consequences on rapid axonal transport.

Although axonal atrophy is usually associated with primary demyelination, including demyelination induced by anti-GC sera (Saida et al., 1979, 1980), this change does not appear to be related to major alterations of rapid axonal transport. Reduction of axonal caliber may be the result of local axon fluid loss (Prineas and McLeod, 1976) or may be due to local alterations of slow axonal transport, as has been proposed to occur during development (Hoffman et al., 1985) and following axotomy (Hoffman et al., 1987).

We conclude that transient focal demyelination, produced by anti-GC sera, did not markedly alter rapid axonal transport. This finding supports clinical observations (for discussion, see Ritchie, 1984b) noting that axons may remain viable while demyelinated. A further implication is that axonal damage, which often occurs coincident with demyelination in disease or toxic states, is not likely to result simply from the absence of myelin, but rather results from additional pathologic factors (see Madrid and Wisniewski, 1976; Said et al., 1981).

References

Aguayo, A. J., G. M. Bray, and C. S. Perkins (1979) Axon-Schwann cell relationships in neuropathies of mutant mice. Ann. NY Acad. Sci. *317:* 512–531.

Benjamins, J. A., R. E. Callahan, I. N. Montgomery, and C. A. Dyer (1986) Production of high titer polyclonal antibodies to galactocerebroside. Trans. Am. Soc. Neurochem. *17:* 146.

Bouldin, T. W., and J. B. Cavanagh (1979) Organophosphorous neuropathy. II. A fine-structural study of the early stages of axonal degeneration. Am. J. Pathol. *94:* 253–262.

Catterall, W. A. (1984) The molecular basis of neuronal excitability. Science *223:* 653–660.

Dyck, P. J., A. C. Lais, S. M. Hansen, M. F. Sparks, P. A. Low, S. Parthasarathy, and W. J. Bauman (1982) Technique assessment of demyelination from endoneurial injection. Exp. Neurol. *77:* 359–377.

Elam, J. S. (1979) Axonal transport of complex carbohydrates. In *Complex Carbohydrates of Nervous Tissue,* R. U. Margolis and R. K. Margolis, eds., pp. 235–267, Plenum, New York.

Fry, J. M., R. P. Lisak, M. C. Manning, and D. H. Silberberg (1976) Serological techniques for detection of antibody to galactocerebroside. J. Immunol. Methods *11:* 185–193.

Goodrum, J. F., and P. Morell (1982) Axonal transport, deposition and metabolic turnover of glycoproteins in the rat optic pathways. J. Neurochem. *38:* 696–704.

Goodrum, J. F., A. D. Toews, and P. Morell (1979) Axonal transport and metabolism of [^{3}H]fucose- and [^{35}S]sulfate-labeled macromolecules in the rat visual system. Brain Res. *176:* 255–272.

Grafstein, B., and D. S. Forman (1980) Intracellular transport in neurons. Physiol. Rev. *60:* 1167–1283.

Griffin, J. W., D. B. Drachman, and D. L. Price (1976) Fast axonal transport in motor nerve regeneration. J. Neurobiol. *7:* 355–370.

Griffin, J. W., D. L. Price, D. B. Drachman, and J. Morris (1981) Incorporation of axonally transported glycoproteins into axolemma during nerve regeneration. J. Cell Biol. *88:* 205–214.

Hall, S. M., and N. A. Gregson (1971) The *in vivo* and ultrastructural effects of injection of lysophosphatidylcholine into myelinated peripheral nerve fibers of the adult mouse. J. Cell Sci. *9:* 769–789.

Hirayama, M., P. A. Eccleston, and D. H. Silberberg (1984) The mitotic history and radiosensitivity of developing oligodendrocytes *in vitro.* Dev. Biol. *104:* 413–420.

Hoffman, P. N., J. W. Griffin, B. G. Gold, and D. L. Price (1985) Slowing of neurofilament transport and the radial growth of developing nerve fibers. J. Neurosci. *5:* 2920–2929.

Hoffman, P. N., D. W. Cleveland, J. W. Griffin, P. W. Landes, N. J. Cowan, and D. L. Price (1987) Neurofilament gene expression: A major determinant of axonal caliber. Proc. Natl. Acad. Sci. USA *84:* 3472–3476.

Hughes, R. A. C., H. C. Powell, S. L. Braheny, and S. Brostoff (1985) Endoneurial injection of antisera to myelin antigens. Muscle Nerve *8:* 516–522.

Kidman, A. D., W. de C. Baker, and H. J. Sippe (1978a) Effect of diphtheric demyelination on axonal transport in the sciatic nerve and subsequent muscle changes in the chicken. Adv. Exp. Med. Biol. *100:* 439–452.

Kidman, A. D., L. Dolan, and H. J. Sippe (1978b) Blockade of fast axonal transport by diphtheritic demyelination in the chicken sciatic nerve. J. Neurochem. *30:* 57–61.

Lowry, O. H., N. J. Rosebrough, A. L. Farr, and R. J. Randall (1951) Protein measurement with the Folin phenol reagent. J. Biol. Chem. *193:* 265–275.

Maizel, J. V. (1971) Polyacrylamide gel electrophoresis of viral proteins. Methods Virol. *5:* 179–246.

Morell, P., R. C. Wiggins, and M. J. Gray (1975) Polyacrylamide gel electrophoresis of myelin proteins: A caution. Anal. Biochem. *68:* 1118–1154.

Morell, P., M. Bornstein, and W. T. Norton (1981) Diseases involving myelin. In *Basic Neurochemistry* 23rd ed., R. W. Albers, G. W. Siegel, R. Katzman, and B. Agranoff, eds., pp. 641–659, Little, Brown, Boston.

Morris, J. H., A. R. Hudson, and G. Weddell (1972) A study of degeneration and regeneration in the divided rat sciatic nerve based on electron microscopy. I. Z. Zellforsch. *124:* 76–102.

Munoz-Martinez, E. J., R. Nunez, and A. Sanderson (1981) Axonal transport: A quantitative study of retained and transported protein fraction in the cat. J. Neurobiol. *12:* 15–26.

Ochs, S. (1975) Retention and redistribution of proteins in mammalian nerve fibres by axoplasmic transport. J. Physiol. (Lond.) *253:* 459–475.

Ochs, S. (1982) *Axoplasmic Transport and its Relation to Other Nerve Functions,* Wiley, New York.

Padilla, S. S., L. J. Roger, A. D. Toews, J. F. Goodrum, and P. Morell (1979) Comparison of proteins transported in different tracts of the central nervous system. Brain Res. *176:* 407–411.

Parhad, I. M., and J. W. Griffin (1986) Fucosyl glycoprotein distribution in the axolemma of the remyelinating peripheral nerve. Soc. Neurosci. Abstr. *12:* 163.

Parhad, I. M., J. W. Griffin, D. L. Price, and D. O. Kuethe (1982) Fucosyl glycoprotein distribution in the demyelinated peripheral nerve. Soc. Neurosci. Abstr. *8:* 28.

Pessoa, V. F., and H. Ikeda (1984) Increase in axonal transport in demyelinating optic nerve fibers in the mouse infected with Semliki Forest virus. Brain *107:* 433–446.

Prineas, J. W., and J. G. McLeod (1976) Chronic relapsing polyneuritis. J. Neurol. Sci. *27:* 427–458.

Ramón y Cajal, S. (1928) *Degeneration and Regeneration of the Nervous System,* pp. 52–55, Oxford University Press, London.

Rao, N. A., J. Guy, and P. S. Sheffield (1981) Effects of chronic demyelination on axonal transport in experimental allergic optic neuritis. Invest. Opthalmol. Vis. Sci. *21:* 606–611.

Ritchie, J. M. (1984a) Physiological basis of conduction in myelinated nerve fibers. In *Myelin,* 2nd ed., P. Morell, ed., pp. 117–141, Plenum, New York.

Ritchie, J. M. (1984b) Pathophysiology of conduction in demyelinated nerve fibers. In *Myelin,* 2nd ed., P. Morell, ed., pp. 337–362, Plenum, New York.

Ritchie, J. M., H. P. Rang, and R. Pellegrino (1981) Sodium and potassium channels in demyelinated and remyelinated mammalian nerve. Nature *294:* 257–259.

Said, G., K. Saida, T. Saida, and A. K. Asbury (1981) Axonal lesions in acute experimental demyelination: A sequential teased nerve fiber study. Neurology *31:* 413–421.

Saida, K., T. Saida, M. J. Brown, D. H. Silberberg, and A. K. Asbury (1978) Antiserum-mediated demyelination *in vivo.* A sequential study

using intraneural injection of experimental allergic neuritis serum. Lab. Invest. *39:* 449–462.

Saida, K., T. Saida, M. J. Brown, and D. H. Silberberg (1979) *In vivo* demyelination induced by intraneural injection of anti-galactocerebroside serum. Am. J. Pathol. *95:* 99–110.

Saida, K., A. J. Sumner, T. Saida, M. J. Brown, and D. H. Silberberg (1980) Antiserum-mediated demyelination: Relationship between remyelination and functional recovery. Ann. Neurol. *8:* 12–24.

Stromska, D., S. Ochs, and J. Muller (1981) Rate of axoplasmic transport in the dystrophic chicken. Exp. Neurol. *74:* 530–547.

Sumner, A. J., K. Saida, T. Saida, D. H. Silberberg, and A. K. Asbury (1982) Acute conduction block associated with experimental antiserum-mediated demyelination of peripheral nerve. Ann. Neurol. *11:* 4690–4770.

Tansey, E. M., and H. Ikeda (1986) The relationship between axonal transport of protein and demyelination in the optic nerves of mice infected with Semliki Forest virus. Brain Res. *397:* 9–15.

Toews, A. D., B. F. Saunders, and P. Morell (1982) Axonal transport and metabolism of glycoproteins in rat sciatic nerve. J. Neurochem. *39:* 1348–1355.

Traugott, U., and C. S. Raine (1984) The neurology of myelin disease. In *Myelin,* 2nd ed., P. Morell, ed., pp. 311–330, Plenum, New York.

Trimmer, P. A., and K. D. McCarthy (1986) Immunocytochemically defined astroglia from fetal, newborn and young adult rats express β-adrenergic receptors *in vitro.* Dev. Brain Res. *27:* 151–165.

Weiss, D. G. (1982) *Axoplasmic Transport,* Springer-Verlag, New York.

Willard, M., W. M. Cowan, and P. R. Vagelos (1974) The polypeptide composition of intra-axonally transported proteins: Evidence for four transport velocities. Proc. Natl. Acad. Sci. USA *71:* 2183–2187.

Williams, M. A. (1977) *Practical Methods in Electron Microscopy,* pp. 77–134, North-Holland, Amsterdam.